Fabrication of hydrophobic drug nanoparticles using a microfluidic spray dryer

Julian Thiele,[a,b] Adam R. Abate,[a] Maike Windbergs,[a] Ho Cheung Shum,[a] Stephan Förster,[b] and David A. Weitz[a‡]

We present a technique for fabricating hydrophobic drug nanoparticles using a microfluidic spray dryer. The nanoparticles are formed by evaporative precipitation of the spray in air at room temperature. Using danazol as a model drug, amorphous nanoparticles are yielded with narrow size distribution, 20-60 nm in diameter. As the device geometry allows us to inject two separate solvent streams, the production of drug co-precipitates with tailor-made composition for optimization of therapeutic efficiency is greatly facilitated.

Introduction

The molecular complexity of drugs has significantly increased over the last decade.[1][2][3] Although molecular complexity usually contributes to biological activity, it often causes poor solubility of drugs.[2][4] This limits their bioavailability and release in the human body, restricting application and commercialization of potential candidates.[5][6] A major approach to increase the bioavailability of a drug is reducing the particle size, which increases the specific surface and, therefore, facilitates release and absorption of the drug.[7][8][9][10]

In this context, spray drying is a powerful technique enabling instantaneous drying of solutions, emulsions or suspensions in one step. The final product is a fine powder with a large surface area. The pharmaceutical application of spray drying techniques covers a broad field ranging from manufacturing dry plant extracts avoiding decomposition of thermo-sensitive components, to the production of excipients for compression with improved binding characteristics.[11][12][13] However, conventional spray dryers often induce high production costs as the fabrication process involves high pressure and complex experimental setups. In addition, particle sizes below 100 nm, as often required for targeted drug delivery, are usually not achievable with commercially available spray dryers.[14][15] These limitations can be overcome using microfluidics.[16][17][18][19][20] A convenient technique to fabricate rather sophisticated microfluidic devices is soft lithography using poly(dimethylsiloxane) (PDMS).[21][22][23] Unfortunately however, hydrophobic compounds easily adsorb onto PDMS microchannels and foul the device.[24][25] An optimal system for fabricating nanoparticles from hydrophobic drugs would combine the versatility of microfluidics with the ability to process hydrophobic drugs by spray drying.

In this paper, we fabricate hydrophobic drug nanoparticles using a microfluidic spray dryer. The device geometry has a high aspect ratio and is rendered hydrophilic by oxygen plasma treatment. This prevents the adsorption of hydrophobic precipitates on the channel walls, thus enabling the use of hydrophobic drugs in PDMS-based microfluidic devices. By controlling the collection distance of the spray, we control the crystallinity of the product. Our microfluidic device enables fabrication of drug nanoparticles less than 100 nm in diameter. The versatile device design also enables the formation of amorphous co-precipitates by co-spray drying the drug with a crystallization inhibitor to improve the bioavailability of hydrophobic drugs.

Results and Discussion

In conventional spray dryers, a single liquid stream is typically vaporized by compressed air in a spray nozzle; the spray is then mixed with a heated gas stream in a drying chamber to evaporate the solvent and yield the dry product.[15] However, this setup only allows processing of single solvent systems or mixtures of premixed solvents. To process multiple separate solvent streams as required for solvent/antisolvent precipitation or rapidly reacting solvent streams, the spray dryer generally needs to be equipped with additional separate inlet channels.[26] In this work, we use a microfluidic device with an array of two flow-focusing cross junctions, as shown in Figure 1.

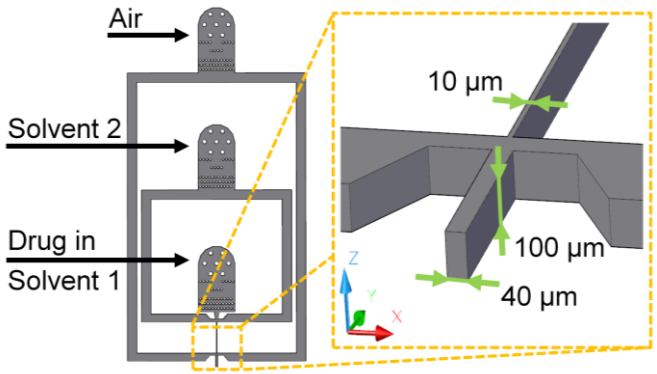

Fig. 1 Schematic of a microfluidic device for forming nanoparticles from hydrophobic drugs by spray drying. The microfluidic device is rendered hydrophilic using oxygen plasma. The device geometry enables separate injection of two solvent streams of which the spray is formed.

The device enables separate injection of two solvents and provides a third inlet for compressed air to form the spray. For the formation of hydrophobic drug nanoparticles, we dissolve the hydrophobic drug in an organic solvent injected into the first inlet, and inject the second fluid into the second inlet. The two solvents form a jet at the first cross junction, which extends into the second cross junction where compressed air is injected to form the spray. To process hydrophobic drugs, the PDMS device must resist fouling due to adsorption of drug crystals on the microchannel walls. We

achieve this by treating the intrinsically hydrophobic PDMS device with oxygen plasma, as the plasma renders the spray dryer hydrophilic.[27] Although the hydrophilicity of the plasma treated device decreases over time, the channel surface can easily be regenerated in the same manner multiple times. To further improve the resistance against fouling, we minimize the surface contact between the drug-loaded solvent stream and the channel walls. We achieve this by designing a device geometry with a high aspect ratio; the ratio *h*/*w* is 10:1 in the upper half of the device and 4:1 at the spray nozzle. As high aspect channels are less pressure-resistant than square channels, the operating spray dryer easily expands, as shown in Figure 2.

To determine the impact of the channel deformation on the flow profile, we process a typical solvent/antisolvent system in our spray dryer and compare the device deformation at low and high pressure. Our observations are supported by computational fluid dynamics (CFD) simulations using COMSOL 4.0a. We design a 3D simulation model considering the structural mechanics of the PDMS channels, the fluid flow described by the Navier-Stokes equations and the diffusion of the solvent streams. For the spray experiment at low pressure, we inject the solvent isopropyl alcohol (IPA), the antisolvent water and compressed air into the first, second and third inlet, respectively, at flow rates of 1 mL h^{-1} for the inner phase and 10 mL h^{-1} for the middle phase. The air pressure is set to 0.34 bar, as shown in Figure 2, left. For the high-pressure experiment, we increase the flow rates of IPA and water to 5 mL h^{-1} and 50 mL h^{-1}, respectively, and set the air pressure to 2.09 bar, as shown in Figure 2, right. At low pressure (0.34 bar), the PDMS device demonstrates minimal deformation and we observe a two dimensional focused flow pattern between the first and second cross junction. However, as we increase the pressure, the PDMS device responds to the internal stress and expands. Due to the high aspect ratio, the strongest expansion of the microchannels is observed in horizontal direction lateral to the fluid flow; the channel walls adapt a quasi-circular shape. This deformation strongly influences the flow profile inside the spray dryer, as shown in Figure 2, bottom. As illustrated by the simulation of the device, the flow profile between the first and second cross junction adopts a three dimensional coaxial flow pattern, similar to that observed in capillaries.[28] Thereby, the inner phase is surrounded by a protective sheath of the middle phase. This minimizes the surface contact of the solvent in which the hydrophobic drug is dissolved with the channel walls and prevents fouling of our spray dryer.

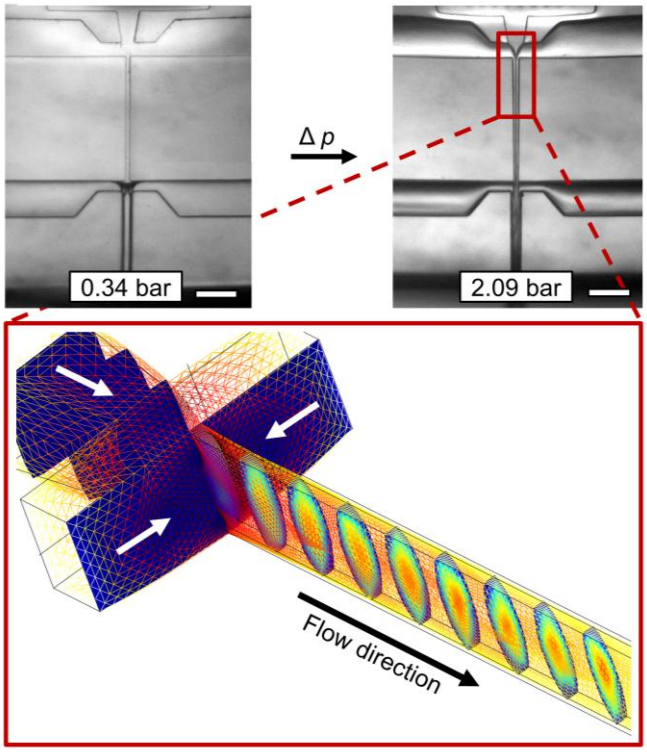

Fig. 2 Pressure-induced deformation of the spray dryer during operation. The impact of the deformation on the flow profile is studied using CFD simulations. The initial rectangular microchannels expand and adopt a quasi-circular shape. This deformation changes the flow pattern from a two dimensional focused flow to a coaxial flow, therefore reducing the contact surface between the drug-loaded solvent stream and the channels walls. The scale bars denote 100 µm.

When forming a spray, the spray shape and drop size are important factors influencing drying, particle size and morphology of the processed drug. To determine drop size and spray shape, we visualize the spray formation in our spray dryer by recording movies with a high-speed camera. We inject IPA into the first and second inlet at a total flow rate of 55 mL h^{-1}. At low air pressure, the solvent stream is not dispersed into a spray; instead, a jet of liquid is ejected from the spray nozzle and breaks into large droplets due to Rayleigh-Plateau instability, as shown in Figure 3a.[28] As the air pressure is increased beyond 0.5 bar, we observe the formation of finely dispersed drops at the spray nozzle, which adopt a round full cone spray pattern. This precise pattern is formed due to turbulences imparted to the liquid prior to the orifice in the short outlet channel. To quantify the spray formation process, we measure the drop size *d* as a function of the air pressure *p*, as shown in Figure 3b. The drop size decreases linearly with increasing pressure to approximately 4 µm in diameter at 2.1 bar, which is the maximum pressure our spray dryer can withstand without delamination of the plasma-bonded PDMS. However, a higher air pressure is easily achievable by increasing the spacing between the microchannels and, therefore, the pressure resistance of the PDMS device.

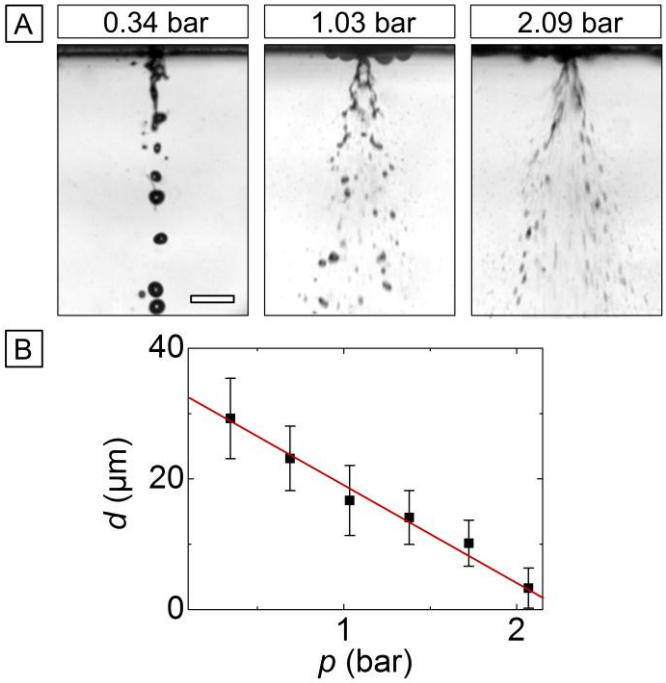

Fig. 3 (a) Spray profile of the nozzle for different air pressures. IPA is injected into the spray dryer at 50 mL h^{-1}. At low pressure, a fluid jet is ejected from the nozzle which breaks into single droplets downstream. When the pressure is increased beyond 0.5 bar, the spray profile adopts full cone spray pattern. The scale bar for all panels denotes 100 µm. (b) Drop diameter as a function of *p*. With increasing pressure, the mean size of the droplets decreases linearly. At a pressure of 2.1 bar, the droplets are approximately 4 µm in diameter. The red line is a guide to the eye.

We demonstrate the concept to form hydrophobic drug nanoparticles with our microfluidic spray dryer. We use danazol as a model drug, which is an isoxazole derivative of testosterone and applied for the treatment of endometriosis and hereditary angioedema.[17] A convenient method for processing hydrophobic drugs is liquid antisolvent precipitation (LASP), where the drug, dissolved in an alcohol, is precipitated by mixing the drug solution with water as the antisolvent.[11][29] We dissolve danazol in isopropyl alcohol and inject it together with water into the first cross junction. As we operate our microfluidic device in the laminar flow regime, only diffusion based mixing of the solvent streams is observed at their interfaces, which does not lead to any precipitation of the drug. To evaluate the sole effect of microfluidic processing on particle size and morphology of the hydrophobic drug, no stabilizer or surfactant is added to influence the particle growth. We set the flow rates to 5 mL h^{-1} for danazol, and 50 mL h^{-1} for water, which corresponds to a volumetric ratio of 1:10 and has been shown to yield danazol microparticles in conventional LASP processes.[17] The spray is completely suspended in air, thus ensuring that the product is dried upon collection. We examine the morphology and particle size of the processed drug by scanning electron microscopy (SEM) analysis. While unprocessed (raw) danazol is composed of particles with irregular shapes ranging from approximately 2 µm to 100 µm, we decrease the particle size significantly by processing the drug using our microfluidic spray dryer. As shown in Figure 4a, we yield danazol nanoparticles with narrow particle size distribution (PSD) from 20 nm to 60 nm and, therefore, smaller than previously reported.[3][17]

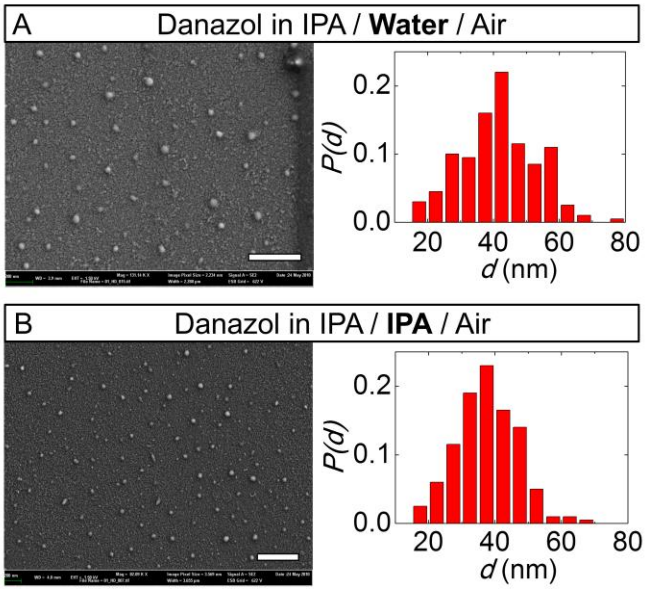

Fig. 4 Effect of the solvent system on particle size and composition. Danazol in IPA is mixed with (a) water as the antisolvent, or (b) IPA as the solvent inside the microfluidic spray dryer. In either cases, nanoparticles are yielded with narrow PSD, 20-60 nm in diameter. Scale bars denote 300 nm.

The formation of drug nanoparticles using LASP is driven by mixing of the drug solution with the antisolvent. Thereby, the degree of supersaturation of the drug solution governs nucleation and growth of the drug nanoparticles.[11] However, sufficient mixing only occurs in the short outlet channel prior to the orifice of the spray nozzle in our microfluidic device. As we use high flow rates to form a stable spray, the delay time of the fluids in the outlet channel should be too short to enable growth of nuclei by mixing. To reveal the formation process, we substitute the antisolvent by the solvent. We inject a solution of danazol in IPA and pure IPA into the first and second inlet, respectively. The formation of danazol nanoparticles of identical size and morphology in the absence of the antisolvent indicates that the particle formation is primarily driven by the evaporation of the spray and not by the formation of nuclei due to supersaturation, as shown in Figure 4b.

Another crucial aspect of the spray drying process is the collection distance of the final product. While it is known that the morphology and size of hydrophobic drugs is dependent on the initial concentration of reactants, the choice of additives and the ratio of solvent and antisolvent,[30] we find a significant dependence on the collection distance by performing spatial sampling of the spray. To illustrate this, we inject danazol together with IPA as previously, but this time we collect the spray in steps of 5 cm from the spray nozzle. SEM analysis is performed revealing two distinct

product morphologies. At a collection distance of 5 cm, we observe a layer-by-layer assembly of danazol; the thickness of each layer is 60 nm to 80 nm, as shown in Figure 5a. These values are in good approximation with the size of single danazol nanoparticles, as shown in Figure 4a and 4b.

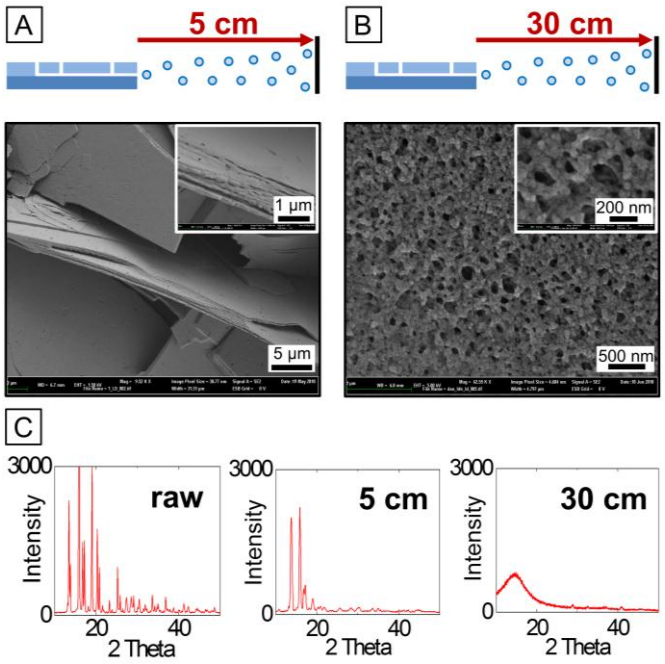

Fig. 5 Spatial sampling of processed danazol. Depending on the collection distance, various morphologies are observed; (a) layer-by-layer assembly, each 60 nm to 80 nm in thickness, and (b) nanoparticles, approximately 20 nm to 60 nm in diameter, assembled in a dense network. (c) XRPD patterns of processed danazol collected at a distance of 5 cm and 30 cm from the spray nozzle, and unprocessed (raw) danazol as a reference.

However, as the time of flight is too short to allow for complete evaporation of the spray upon collection, the remaining solvent increases the mobility of particles on the collection substrate, allowing them to fuse and reach an energetically more favorable state.[11] We therefore increase the collection distance to 30 cm; as the spray is completely evaporated, single nanoparticles are formed, as shown in Figure 5b. X-ray powder diffraction analysis (XRPD) is employed to determine the effect of spatial sampling on the crystallinity of danazol. We use the characteristic peaks at 2θ of 15.8, 17.1 and 19.0 in the XRD pattern of unprocessed danazol as reference. In processed danazol, the intensity of the characteristic peaks decreases as the collection distance of the spray is increased. This indicates that the initial crystallinity of the drug is not recovered, as shown in Figure 5c. The formation of amorphous danazol is of importance, as the difference in physicochemical properties of the amorphous form significantly increases the bioavailability of danazol.[17]

Another way to fabricate amorphous hydrophobic drug particles is to co-spray dry the drug and a crystallization inhibitor.[31] To demonstrate this using our microfluidic spray dryer, we perform two experiments. We co-spray dry danazol in IPA together with water and collect the spray at low distance. As shown before, the spray is not completely evaporated due to the short time of flight. This allows danazol to grow into star-shape crystalline aggregates, as shown in Figure 6a. However, by using a crystallization inhibitor, amorphous danazol is formed. We use poly(vinylpyrrolidone) (PVP), which is well known to inhibit crystal growth in pharmaceutical formulations.[32][33][34][35] We process danazol in IPA together with a 1.5 wt% solution of PVP in water at equal flow rates of 25 mL h^{-1}, as shown in Figure 6b. Again, the spray is collected at short distance. However, as the spray is dried, danazol precipitates from the spray in a PVP matrix without crystallization, thus no characteristic peaks are observed in the XRPD pattern.

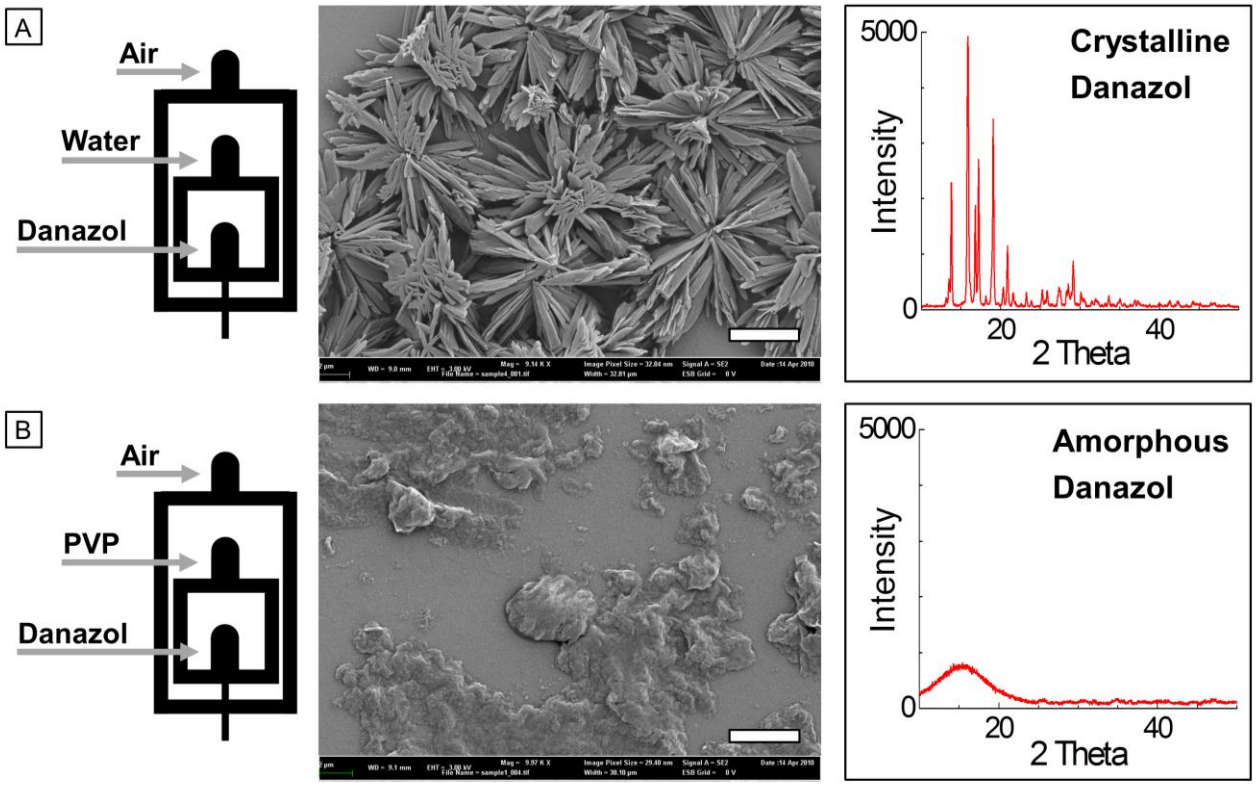

Fig. 6 Inhibition of danazol crystallization by PVP. (a) Danazol in IPA is mixed with water inside the microfluidic device; the spray is collected at a distance of 5 cm from the nozzle, allowing danazol to grow into crystalline aggregates, as indicated by the XRPD pattern. (b) By processing danazol in IPA and an aqueous solution of PVP, which are injected separately into our spray dryer, amorphous co-precipitates are yielded, as indicated by the XRPD pattern. Scale bars denote 5 µm.

To demonstrate the advantages of our microfluidic spray dryer, we perform spray drying experiments with the same formulations in a conventional laboratory spray dryer and compare the results by XRPD and SEM. We use a Mini Spray Dryer B 191 (Büchi, Germany) with a spray rate of 10 mg min^{-1}, and process a solution of danazol in IPA as well as a solution of danazol in IPA together with PVP. In the former case, we yield particles ranging from approximately 1 µm to 5 µm, and, therefore, substantially larger than the danazol particles formed with our microfluidic spray dryer. Moreover, the crystallinity of danazol is retained, as shown in Figure 7a. Similar results are observed for the formation of co-precipitates of danazol and PVP, as shown in Figure 7b. Although the initial crystallinity of danazol is suppressed by PVP, the particles are again two orders of magnitude larger than in comparable experiments using our microfluidic device.

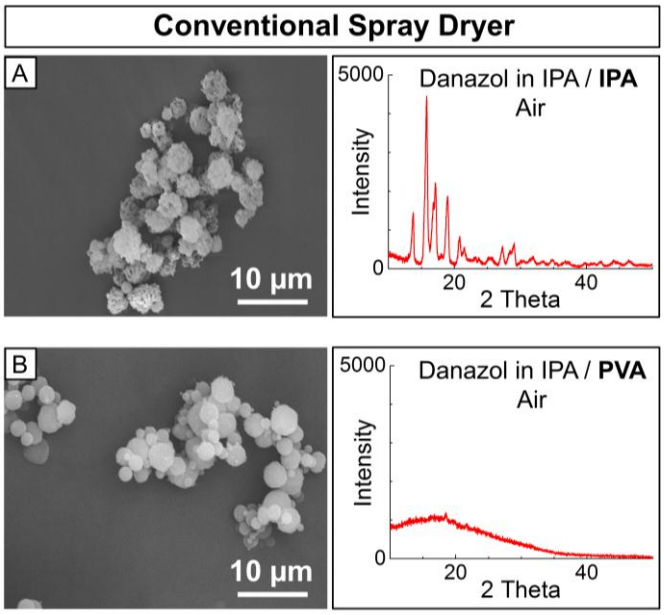

Fig. 7 Fabrication of danazol particles and danazol/PVP co-precipitates in a conventional spray dryer using the same formulations as in our microfluidic device. (a) Instead of amorphous drug nanoparticles, crystalline microparticles, and (b) microscopic co-precipitates are yielded.

Experimental

Device Fabrication

The PDMS microfluidic devices are fabricated using soft lithography.[21] All channels have a fixed height of 100 µm. The PDMS replica is bonded to a flat sheet of cured PDMS using oxygen plasma treatment. The plasma treatment renders the microchannels temporarily hydrophilic.[27] To retain the hydrophilic surface modification, suitable for handling hydrophobic drugs, the device is flushed with deionized water. The nozzle of the spray dryer is prepared by slicing the outlet channel of the stamped device with a razor blade. To achieve reproducible accuracy when slicing, we include a guide to the eye in the initial AutoCAD design of the spray dryer.

Spray drying experiments

PVP (weight-averaged molecular weight, M_W 10,000 g mol^{-1}) and all other chemicals are obtained from Sigma-Aldrich Co. unless noted otherwise. Danazol (99.9 %) is obtained from Selectchemie AG. Water with a resistivity of 16.8 MΩcm^{-1} is prepared using a Millipore Milli-Q system. All solutions are filtered through a 0.2 µm PTFE filter (Millipore). We form danazol nanoparticles using our microfluidic spray dryer. To demonstrate long term stability of the process, each experiment is performed over a time period of 2 h. We inject a saturated solution of danazol in IPA into the first inlet and water or IPA into the second inlet at 5 mL h^{-1} and 50 mL h^{-1}, respectively. For the formation of co-precipitates, we inject PVP in water (1.5 % w/w) at 50 mL h^{-1} into the second inlet. To form the spray, air is injected into the third inlet at 2.1 bar. The spray is ejected into air and dried at room temperature; the yield ranges from 70 % to 95 %. We image the spray using a Phantom v9.1 camera (Vision Research) at 64,000 fps. The droplet size is obtained by measuring the size of at least 200 drops from high-speed camera images.

Product collection and characterization

Processed danazol is collected at distances between 5 cm and 30 cm from the spray nozzle. For SEM analysis, the spray is collected on glass slides and coated with Pd/Pt. We use an Ultra55 Field Emission SEM (Zeiss). The size distribution of the nanoparticles is determined by image analysis of SEM photographs using ImageJ. For XRPD analysis, samples are collected in an aluminium box over which the spray dryer is mounted. XPRD analysis is performed using a Scintag XDS2000 powder diffractometer (Scintag, Cupertino, California, USA) with Cu Kα radiation at 40 kV and 30 mA. The XRD patterns are taken at room temperature in the range of $10° \leq 2\theta \leq 50°$ with a scan rate of 1° min^{-1} and a step size of 0.02°.

Conclusions

Our microfluidic spray dryer allows us to form nanoparticles from hydrophobic drugs. As shown for our model drug danazol, amorphous nanoparticles are yielded with narrow size distribution and lowest reported mean particle size. Due to the hydrophilic surface treatment and the high aspect ratio of the microchannels, fouling of the microfluidic device is prevented. This allows for application of the spray drying approach for nanoparticles to a wider range of hydrophobic drugs and creates new opportunities for the development of commercial formulations of water-insoluble drugs. As the spray is dried at room temperature, our microfluidic device also enables processing of thermo-sensitive materials. By independent injection of two solvent streams, co-precipitates of hydrophobic drugs can be prepared. As the two solvent streams do not mix before spray formation, our device also enables spray drying of rapidly reacting compounds. Our approach should also be useful for forming composite nanoparticles with freely tunable composition. In addition, nanosuspensions, which greatly enhance the dissolution rate and bioavailability of hydrophobic drugs, can be easily prepared by spraying the nanoparticles into a stabilizer solution.[2][11]

Acknowledgements

We thank Christian Holtze and Jim Wilking for helpful discussions, and Martin Trebbin for designing the CFD model. This work was supported by BASF, the NSF (DMR-0602684), the Harvard MRSEC (DMR-0820484), and the Massachusetts Life Sciences Center. Experiments were performed in part at the Center for Nanoscale Systems (CNS), which is supported by the NSF (ECS-0335765). JT received funding from the Fund of the Chemical Industry (Germany) and MW was funded by the German Academic Exchange Service.

Notes and references

[a] *School of Engineering and Applied Sciences/Department of Physics, Harvard University, Cambridge, Massachusetts, USA. 617-495-3275; E-mail: weitz@seas.harvard.edu*
[b] *Physical Chemistry I, University of Bayreuth, Germany*
‡ Corresponding author
† Electronic Supplementary Information (ESI) available: [High speed imaging of spray formation].

[1] X. Chen, J. M. Vaughn, M. J. Yacaman, R. O. Williams III, K. P. Johnston, *Journal of Pharmaceutical Sciences*, 2004, **93**, 1867-1878.
[2] B. E. Rabinow, *Nature Reviews Drug Discovery*, 2004, **3**, 785-796.
[3] T. Panagiotou, S. V. Mesite, R. J. Fisher, *Industrial and Engineering Chemistry Research*, 2009, **48**, 1761-1771.
[4] A. Schuffenhauer, N. Brown, P. Selzer, P. Ertl, E. Jacoby, *Journal of Chemical Information and Modeling*, 2006, **46**, 525-535.
[5] N. Rasenack, B. W. Müller, *Pharmaceutical Research*, 2002, **19**, 1894-1900.

[6] C. A. Lipinski, *American Pharmaceutical Review*, 2002, **5**, 82-85.
[7] P. Costa, J. M. S. Lobo, *European Journal of Pharmaceutical Sciences*, 2001, **13**, 123-133.
[8] L. Gao, D. Zhang, M. Chen, *Journal of Nanoparticle Research*, 2008, **10**, 845-862.
[9] E. Merisko-Liversidge, G. G. Liversidge, E. R. Cooper, *European Journal of Pharmaceutical Sciences*, 2003, **18**, 113-120.
[10] F. Kesisoglou, S. Panmai, Y. Wu, *Advanced Drug Delivery Reviews*, 2007, **59**, 631-644.
[11] R. Vehring, *Pharmaceutical Research*, 2008, **25**, 999-1022.
[12] D. Chiou, T. A. G. Langrish, R. Braham, *Journal of Food Engineering*, 2008, **86**, 288-293.
[13] Y. Gonnisson, S. I. Goncalves, J. P. Remon, C. Vervaet, *Drug Development and Industrial Pharmacy*, 2008, **34**, 248-257.
[14] H. Gao, W. Shi, L. B. Freund, *Proceedings of the National Academy of Sciences*, 2005, **102**, 9469-9474.
[15] X. Li, N. Anton, C. Arpagaus, F. Belleteix, T. F. Vandamme, *Journal of Controlled Release*, 2010, doi:10.1016/j.jconrel.2010.07.113.
[16] H. S. M. Ali, P. York, N. Blagden, *International Journal of Pharmaceutics*, 2009, **375**, 107-113.
[17] H. Zhao, J.-X. Wang, Q.-A. Wang, J.-F. Chen, J. Yun, *Industrial and Engineering Chemistry Research*, 2007, **46**, 8229-8235.
[18] G. Tetradis-Meris, D. Rossetti, C. P. de Torres, R. Cao, G. Lian, R. Janes, *Industrial and Engineering Chemistry Research*, 2009, **48**, 8881-8889.
[19] P. W. Miller, L. E. Jennings, A. J. deMello, A. D. Gee, N. J. Long, R. Vilar, *Advanced Synthesis and Catalysis*, 2009, **351**, 3260-3268.
[20] A. S. Utada, E. Lorenceau, D. R. Link, P. D. Kaplan, H. A. Stone, D. A. Weitz, *Science*, 2005, **308**, 537-541; J. Thiele, D. Steinhauser, T. Pfohl, S. Förster, *Langmuir*, 2010, **26**, 6860-6863; Y. Wang, W.-Y. Lin, K. Liu, R. J. Lin, M. Selke, H. C. Kolb, N. Zhang, X.-Z. Zhao, M. E. Phelps, C. K. F. Shen, K. F. Faull, H.-R. Tseng, *Lab on a Chip*, 2009, **9**, 2281-2285.
[21] Y. Xia, G. M. Whitesides, *Angewandte Chemie International Edition*, 1998, **37**, 550-575; D. Duffy, J. McDonald, O. Schueller, G. M. Whitesides, *Analytical Chemistry*, 1998, **70**, 4974-4984.
[22] S. L. Peterson, A. McDonald, P. L. Gourley, D. Y. Sasaki, *Journal of Biomedical Materials Research Part A*, 2004, **72A**, 10-18.
[23] D. B. Weibel, G. M. Whitesides, *Current Opinion in Chemical Biology*, 2006, **10**, 584-591.
[24] P. Mayer, W. H. J. Vaes, J. L. M. Hermens, *Analytical Chemistry*, 2000, **72**, 459-464.
[25] M. Honest, H. K. Jin, L. Kwanseop, P. Nokyoung, H. H. Jong, *Electrophoresis*, 2003, **24**, 3607-3619.
[26] T. Ozeki, S. Beppu, T. Mizoe, Y. Takashima, H. Yuasa, H. Okada, *Pharmaceutical Research*, 2006, **23**, 177-183; T. Ozeki, S. Beppu, T. Mizoe, Y. Takashima, H. Yuasa, H. Okada, *Journal of Controlled Release*, 2005, **107**, 387-394.
[27] B. Kim, E. T. K. Peterson, I. Papautsky, *Proceedings of the 26th Annual International Conference of the IEEE EMBS*, San Francisco, 2004, 5013-5016; D. Bodas, C. Khan-Malek, *Microelectronic Engineering*, 2006, **83**, 1277-1279.
[28] A. S. Utada, L.-Y. Chu, A. Fernandez-Nieves, D. R. Link, C. Holtze, D. A. Weitz, *Materials Research Society Bulletin*, 2007, **32**, 702-708.
[29] J.-Y. Zhang, Z.-G. Shen, J. Zhong, T.-T. Hu, J.-F. Chen, Z.-Q. Ma, J. Yun, *International Journal of Pharmaceutics*, 2006, **323**, 153-160.
[30] S. D. Škapin, E. Matijević, *Journal of Colloid and Interface Science*, 2004, **272**, 90-98.
[31] S. M. Wong, I. W. Kellaway, S. Murdan, *International Journal of Pharmaceutics*, 2006, **317**, 61-68.
[32] H. Sekikawa, M. Nakano, T. Arita, *Chemical and Pharmaceutical Bulletin*, 1978, **26**, 118-126.
[33] M. Yoshioka, B. C. Hancock, G. Zografi, *Journal of Pharmaceutical Sciences*, 1995, **84**, 983-986.
[34] L. S. Taylor, G. Zografi, *Pharmaceutical Research*, 1997, **14**, 1691-1698.
[35] J.-H. Kim, H.-K. Choi, *International Journal of Pharmaceutics*, 2002, **236**, 81-85.

Table of content:

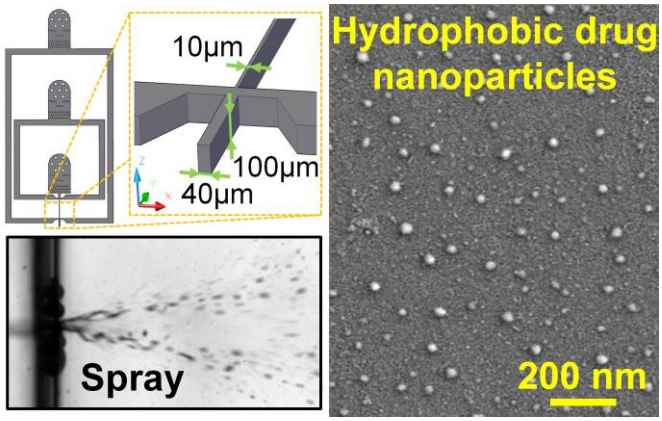

A novel microfluidic spray dryer for fabricating nanoparticles from hydrophobic drugs is described. The nanoparticles are formed without additives at room temperature and yielded with low mean particle size. By separate injection of two solvent streams, co-precipitates with freely tunable composition can be formed.